THREE-DIMENSIONAL MATHEMATICAL MODEL FOR SIMULATING THE HYDROLOGIC SYSTEM IN THE PICEANCE BASIN, COLORADO

U. S. GEOLOGICAL SURVEY

Water-Resources Investigations
Open-File Report 82-637

Prepared in cooperation with the
Colorado River Water Conservation District
United States Department of Energy

THREE-DIMENSIONAL MATHEMATICAL MODEL FOR SIMULATING THE HYDROLOGIC SYSTEM IN THE PICEANCE BASIN, COLORADO

by O. James Taylor

U.S. GEOLOGICAL SURVEY

Water-Resources Investigations

Open-File Report 82-637

Prepared in cooperation with the

COLORADO RIVER WATER CONSERVATION DISTRICT and the

U.S. DEPARTMENT OF ENERGY

1982

UNITED STATES DEPARTMENT OF THE INTERIOR

JAMES G. WATT, Secretary

GEOLOGICAL SURVEY

Dallas L. Peck, Director

For additional information
write to:

District Chief
U.S. Geological Survey
Box 25046, Mail Stop 415
Denver Federal Center
Lakewood, CO 80225

CONTENTS

ILLUSTRATIONS
[Plates are in pocket]

CONTENTS

TABLES

METRIC CONVERSION FACTORS

For the reader who may prefer to use metric (SI) units rather than inch-pound units, the conversion factors for the terms used in this report are listed below:

Multiply inch-pound units	*By*	*To obtain metric units*
barrel	1.59×10^{-1}	cubic meter
British thermal unit per hour per foot per degree Fahrenheit (Btu/hr/ft/°F)	4.04×10^{-3}	calorie per second per centimeter per degree Celsius
cubic foot per second (ft^3/s)	2.832×10^{-2}	cubic meter per second
cubic mile (mi^3)	4.166	cubic kilometer
foot (ft)	3.048×10^{-1}	meter
foot per day (ft/d)	3.048×10^{-1}	meter per day
gallon per ton (gal/ton)	4.171×10^{-2}	cubic meter per megagram
inch (in.)	25.4	millimeter
inch per year (in./yr)	25.4	millimeter per year
square foot (ft^2)	9.290×10^{-2}	square meter
square foot per day (ft^2/d)	9.290×10^{-2}	square meter per day
square mile (mi^2)	2.590	square kilometer

National Geodetic Vertical Datum of 1929 (NGVD of 1929): A geodetic datum derived from a general adjustment of the first-order level nets of both the United States and Canada, formerly called *"Mean Sea Level."*

THREE-DIMENSIONAL MATHEMATICAL MODEL FOR SIMULATING THE HYDROLOGIC SYSTEM IN THE PICEANCE BASIN, COLORADO

By O. James Taylor

ABSTRACT

The Piceance basin extends over an area of about 1,600 square miles in northwestern Colorado and includes the drainage basins of Piceance, Yellow, Roan, and Parachute Creeks. Beneath the drainage basins lie the Uinta and Green River Formations of Eocene age and older rocks. The Uinta and Green River Formations consist of marlstone, sandstone, and siltstone and include large reserves of oil shale. Extensive fracturing and leaching of the formations has increased their permeability and resulted in aquifers that lie within, above, and below the oil-shale deposits.

The hydrologic system of the basin consists of natural recharge from precipitation, circulation through fractured aquifers and confining beds, and discharge to stream valleys or seepage faces. Previous models were utilized to simulate the flow systems in the northern part of the Piceance basin. A preliminary three-dimensional, five-layer simulation model was prepared for the entire basin using available hydrologic data. The model was used in a steady-state error analysis to assess the degree of error in the hydrologic parameters used in the model. This analysis indicated that simulated hydrologic characteristics are plausible, all layers exhibit impaired vertical hydraulic conductivity, and one layer may exhibit lateral directional transmissivity. However, the model could not be calibrated because of the paucity of data in some regions of the basin.

INTRODUCTION

Location and general hydrogeology of study area

The Piceance basin is part of a structural basin in northwestern Colorado. The study area, shown in figure 1, lies within the structural basin. Normal annual precipitation ranges from 12 to 20 in.; larger amounts fall at higher altitudes where more than half of the precipitation accumulates as snow. Two major drainage basins are shown in figure 2. Yellow and Piceance Creeks are tributary to the White River and drain the northern part of the basin. Roan and Parachute Creeks are tributary to the Colorado River and drain the southern part of the basin. Total area of the drainage basins shown in figure 2 is about 1,600 mi^2.

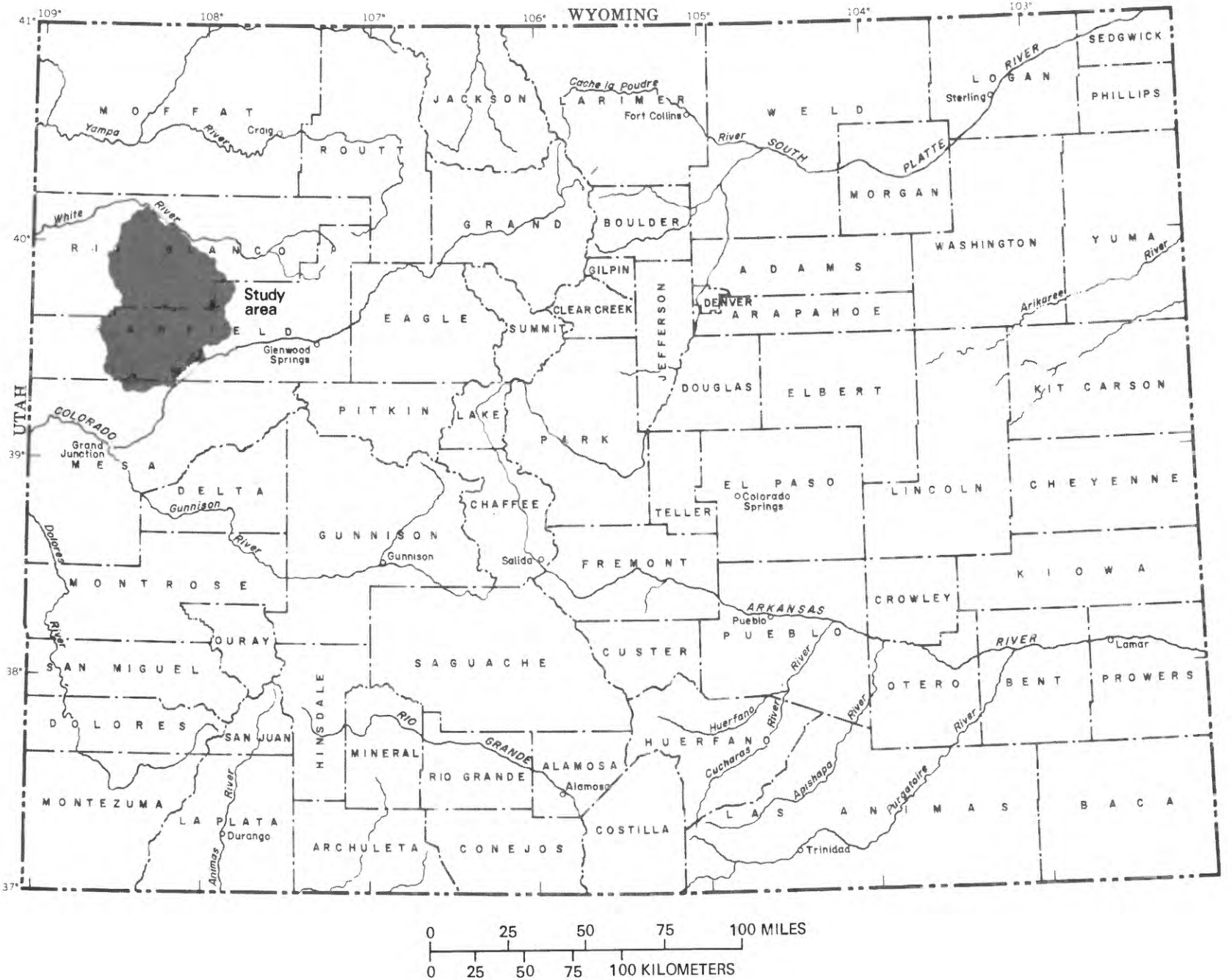

Figure 1.--Location of study area.

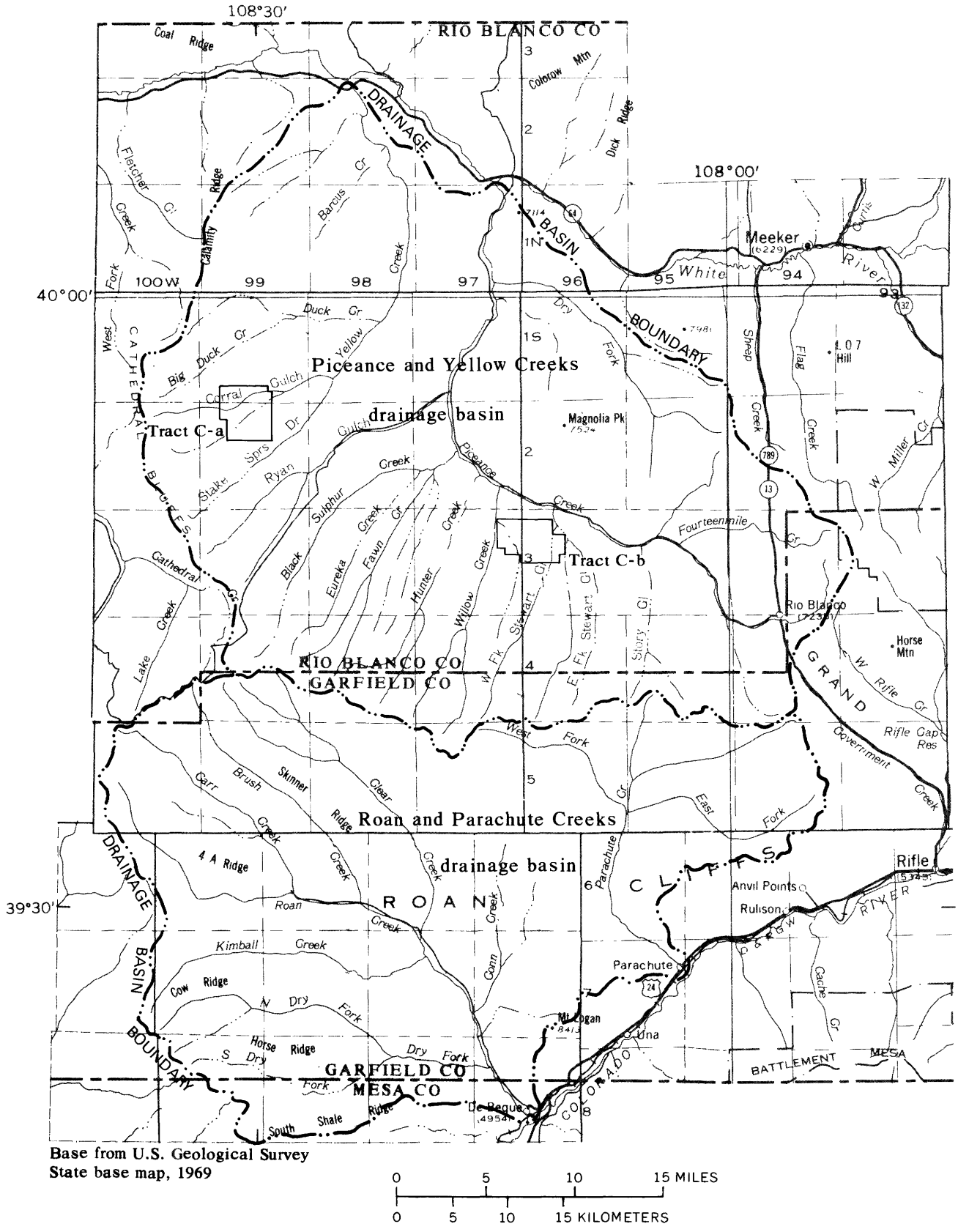

Figure 2.--Major drainage basins of the Piceance basin, northwestern Colorado.

Water occurs in aquifers of various types. Alluvial aquifers consisting of gravel, sand, and clay and having a maximum thickness of 140 ft lie along the stream valleys. Because of the presence of clay beds in some reaches of the alluvium, ground water occurs under both confined and unconfined conditions (Coffin and others, 1968). A few holes penetrating the alluvium are reported dry; however, in most reaches of the stream valleys, ground water moves as underflow in the alluvium below the stream channels. The alluvial aquifers are of smaller extent than the bedrock aquifers.

The principal bedrock aquifers occur within the Uinta and Green River Formations of Eocene age. The Uinta Formation consists of fractured sandstone, marlstone, and siltstone that contain ground water in porous or fractured beds. The underlying Green River Formation is subdivided into members that include the Parachute Creek Member and the Garden Gulch Member, as shown in figure 3. The Parachute Creek Member consists of fractured marlstone and leached zones that contain ground water and include oil-shale zones. The Mahogany zone of the Parachute Creek Member of the Green River Formation is a layer rich in oil shale in which the oil concentration is 15 to 30 gal/ton (Pitman and Johnson, 1978). Other rich oil-shale zones are shown in figure 3 with R- prefixes, separated by lean zones shown with L- prefixes (Cashion and Donnell, 1972). Concentration of oil in the R-6 zone ranges from 5 to 30 gal/ton (Pitman, 1979). The Garden Gulch Member is a relatively impermeable marlstone, shale, and sandstone layer that forms the base of the aquifer system shown in figure 3. In the eastern part of the basin the Anvil Points Member of the Green River Formation is the relatively impermeable equivalent of the lower Parachute Creek Member, Garden Gulch Member, and underlying Douglas Creek Member. However, a zone in the lower part of the Parachute Creek Member in the north-central part of the basin consists of relatively impermeable and probably unfractured marlstone that contains saline minerals. This zone is known as the high-resistivity zone and ranges from 200 to 900 ft in thickness (Coffin and others, 1971). Accordingly, the base of the aquifer system lies stratigraphically above the top of the Garden Gulch Member in the north-central part of the basin. Above the high-resistivity zone lies the low-resistivity or leached zone that has been fractured. Circulating ground water has leached soluble minerals from the low-resistivity zone and resulted in relatively high permeability. For convenience, the bedrock aquifers above the Mahogany zone are referred to herein as the upper aquifers. Aquifers below the Mahogany zone and above the Garden Gulch Member or equivalent beds are referred to as the lower aquifers.

Oil-Shale Development and Mine Drainage

Oil-shale resources in the Piceance basin are large. Estimates of the quantity of oil in place in the basin depend on the grade of oil shale considered, according to the Federal Energy Administration (1974):

Minimum grade of oil shale (gallons per ton)	Volume of oil (barrels)
30	0.355×10^{12}
25	$.607 \times 10^{12}$
15	1.200×10^{12}

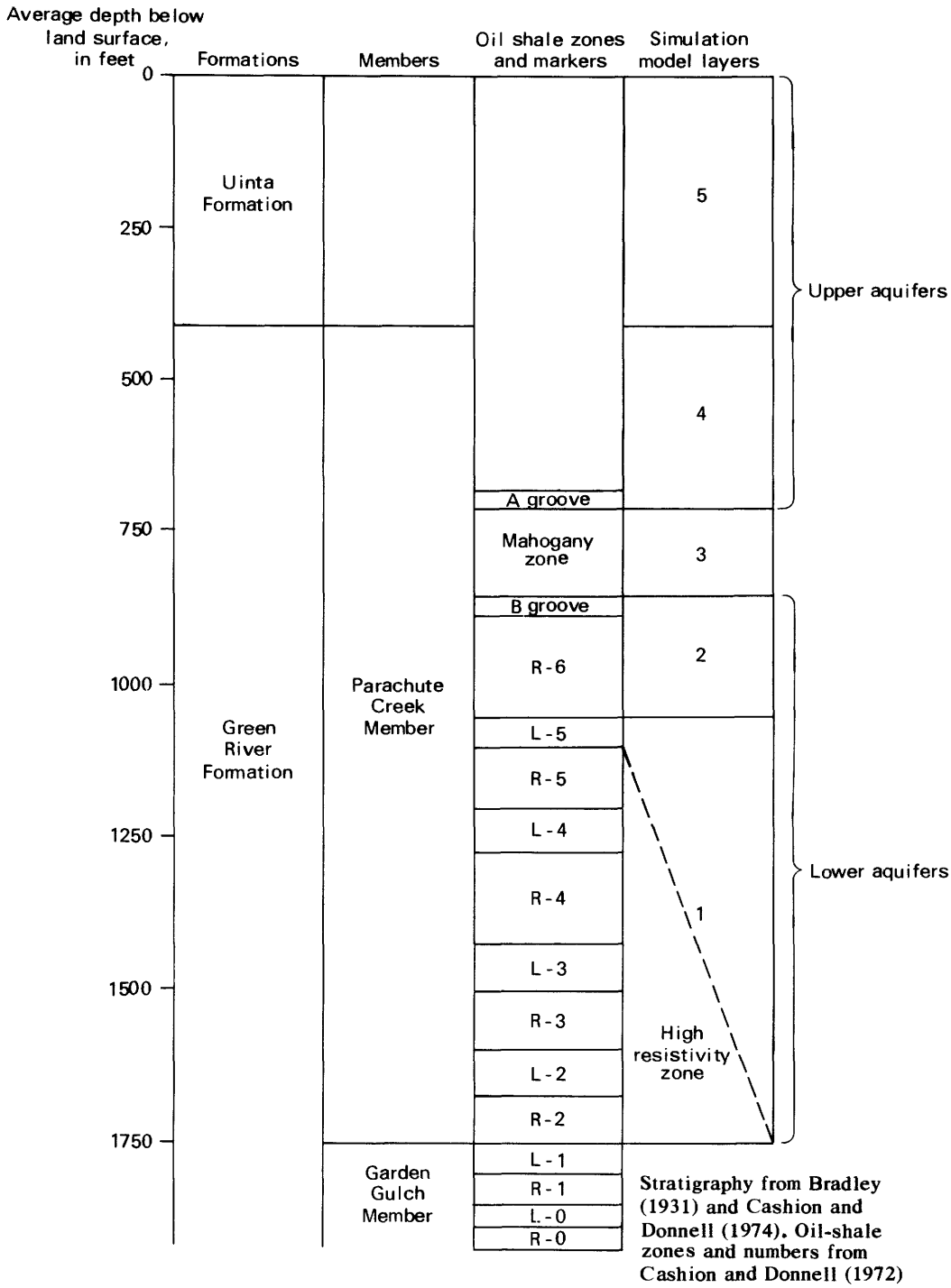

Figure 3.-- Generalized correlation of stratigraphic, oil-shale, and simulation model layers, Piceance basin, northwestern Colorado.

The volume of oil in place is estimated to be more than 1 trillion barrels if all deposits having an average grade equal to or greater than 15 gal/ton are considered. The amount of recoverable oil depends on the methods of mining and retorting.

Many private companies and the U.S. Department of Energy are in the process of exploring and developing oil-shale resources at numerous sites in the basin. Mining rights are derived from leases and mineral claims on Federal land, as well as on fee (private) land. Drainage of most oil-shale mines will be required because of the occurrence of ground water above, within, and below the oil-shale deposits. Drainage of the mines will insure mine safety and permit in-situ retorting, if desired. Drainage of the mines also will provide water supplies that may be suitable for plant requirements.

Purpose and Scope

Oil-shale development depends on many technologies, including water-resources technology. The purpose of this report is to describe analyses of the hydrologic system in the Piceance basin. These analyses were conducted by preparing a three-dimensional computer model of the basin and using the model to evaluate reasonable ranges in aquifer properties. This study incorporates concepts of the aquifer properties and hydrologic systems developed in various model studies. This study is part of ongoing hydrologic data-collection and analysis programs in the basin.

The model described by Weeks and others (1974) utilized about 1,600 nodes to predict the hydrologic impact of mine drainage under transient conditions at tracts C-a and C-b. This model was uncalibrated. The model described by Robson and Saulnier (1981) utilized about 600 nodes to predict the hydrologic and mass-transport impacts of mine drainage at the two tracts, also under transient conditions. This model employed a steady-state calibration utilizing potentiometric heads, dissolved-solids concentration in model layers, and the quantity and quality of water discharged from the aquifers.

The model described herein considers the hydrologic system that underlies the drainage basins of Piceance, Yellow, Roan, and Parachute Creeks. The aquifers and confining beds were subdivided into the five simulation-model layers shown in figure 3. These layers, serially numbered in ascending order, were used in the simulation-model studies described in the section entitled, "Mathematical Model." Valley-fill alluvial aquifers that lie stratigraphically above the Uinta Formation are not included in the model studies.

The model described in this report employs a network of 6,085 active nodes in the expanded region. A preliminary calibration under steady-state conditions utilized potentiometric heads and natural discharge to streams. The new model was developed by extrapolating over the Piceance basin meager hydrologic data compiled from field tests and published reports. The estimated level of error in the model can be regarded as tolerable until more field data are available. As additional field data become available, they will be incorporated into the model and the model capability will be expanded.

HYDROLOGIC SYSTEM

Hydrogeologic Framework

The attitudes of the aquifers and confining layers described are controlled by a northerly tilted structural basin. Structure contour maps prepared by Coffin and others (1971), Pitman and Johnson (1978), and Pitman (1979) indicate that the Mahogany zone of the Parachute Creek Member of the Green River Formation is about 3,900 ft lower in the northern part of the basin than in the southwestern part. Numerous folds and normal faults are apparent from the structure contour maps and the geologic map prepared by Donnell (1961). The Uinta Formation is exposed over most of the basin; the Green River and older formations are exposed in the basin margins and in numerous incised valleys within the drainages of Roan and Parachute Creeks.

Fractures are common in the aquifers and less common in the Mahogany zone. Fractures are important hydrologically because ground water moves more readily through the fractures than through the pores of the rock. Therefore, the permeability is mostly due to fractures, and directional trends in fractures will cause directional variations in permeability. A fracture map based on aerial photographs prepared by Welder (1971) for the Piceance Creek basin suggests that most surface fractures trend northwest. An extensive inventory of 5,107 joints in outcrops at 40 field sites in the Piceance Creek basin is described by Smith and Whitney (1979). As many as three major joint sets were identified at each field site and a total of 3,114 joints was included in the major joint sets. A circular frequency diagram (fig. 4) shows the number and direction of joints in the major sets. The prominent trend shown in the diagram averages about N 75° W; other trends are much less prominent. The simulation model described later in this report was designed to account for the anisotropy of the hydraulic conductivity, suspected because of the predominance of surface fractures along a directional trend.

The solutional zones in the lower aquifers also are important hydrologically because they widened the fractures, thereby increasing the permeability, porosity, and specific yield of affected zones. The solutional activity, as evidenced by vuggy zones, probably served to change the hydraulic characteristics of the lower aquifers in comparison to the upper aquifers.

Recharge, Ground-Water Movement, and Discharge

Land-surface altitudes in the Piceance basin range from about 5,600 ft along the White River to about 9,000 ft in the drainage divide between Roan and Parachute Creeks. Natural recharge results from the slow melting of a relatively thick snowpack above 7,000-ft altitudes, according to Weeks and others (1974). From 1931 to 1960, normal winter (October-April) precipitation ranged from about 6 in./yr at low altitudes to 12 in./yr at high altitudes, according to the U.S. Weather Bureau (1960). Ground-water flow systems are shown schematically in figure 5.

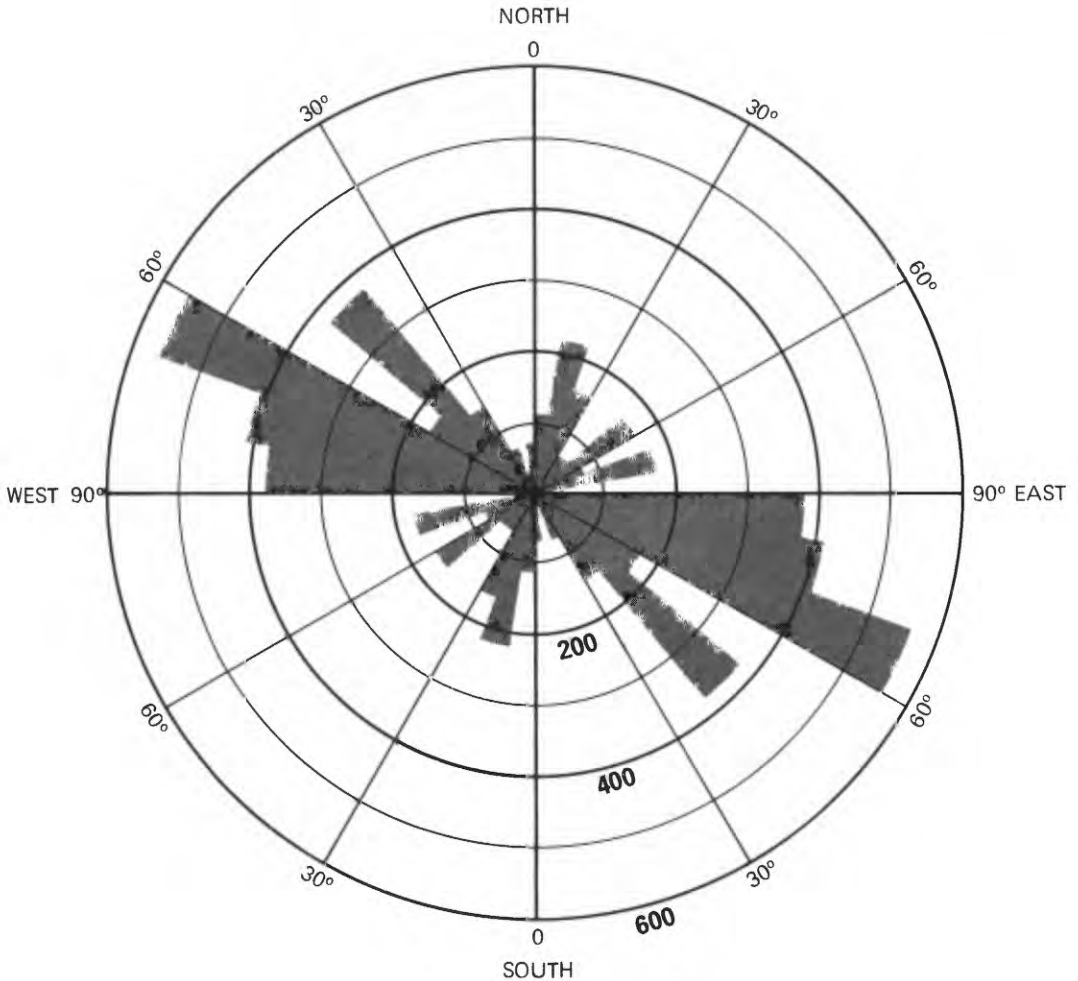

Figure 4.-- Circular frequency diagram for trends of surface fractures.

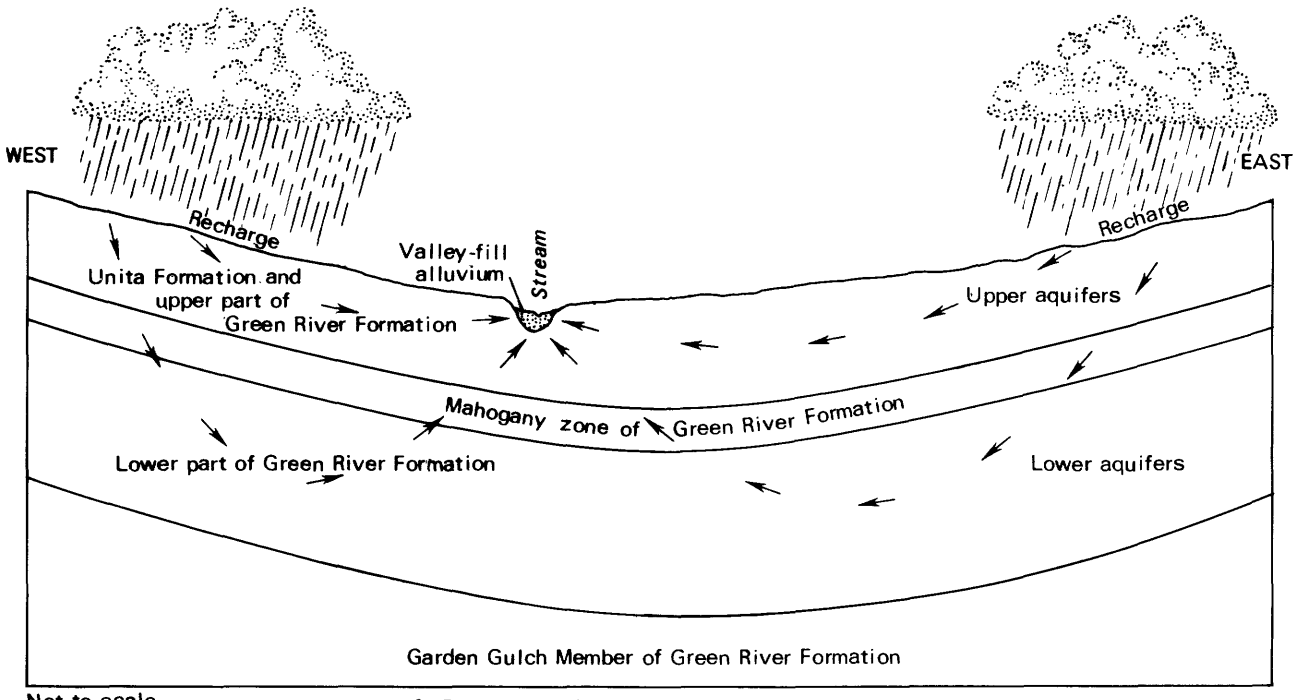

A. Piceance and Yellow Creek drainage basins

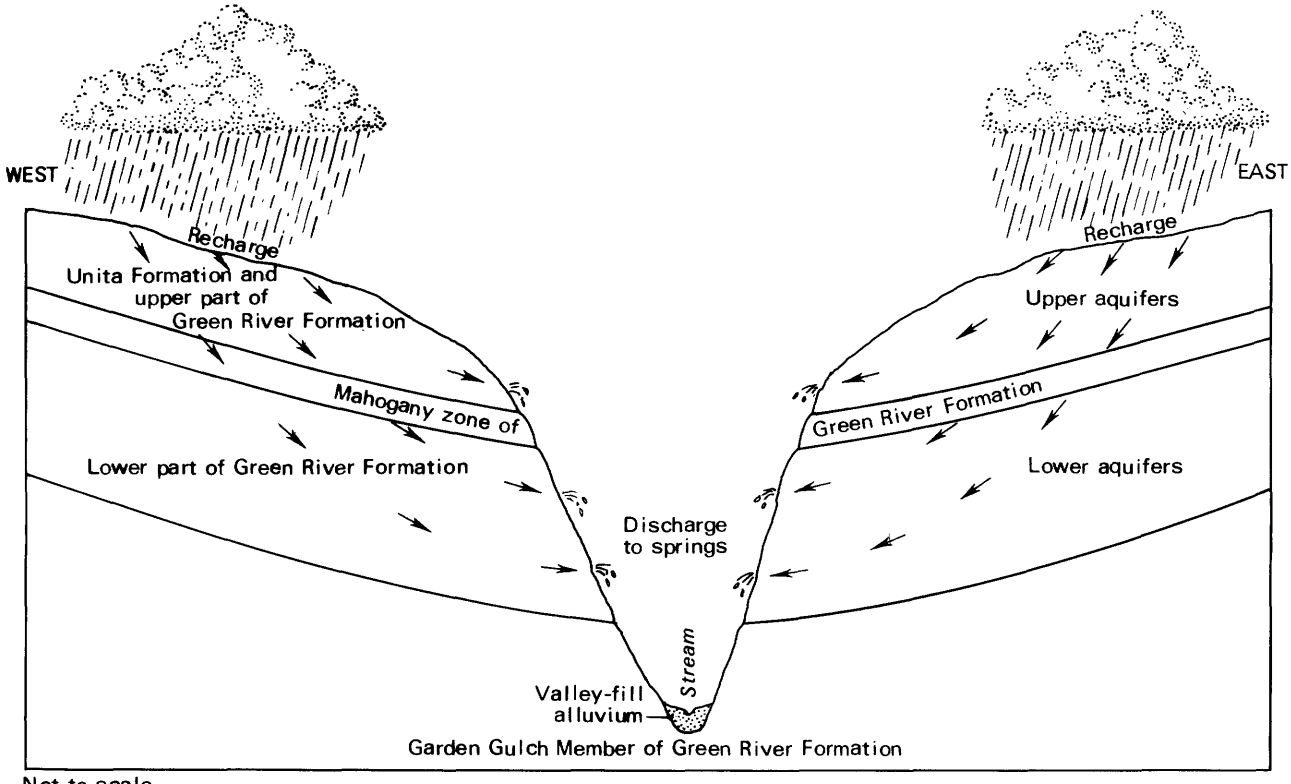

B. Roan and Parachute Creek drainage basins

Figure 5.--Schematic diagram of ground-water flow systems.

In the drainage basins of Piceance and Yellow Creeks, part of the recharged water flows through the upper aquifers to major streams. Part of the recharged water flows downward through the relatively impervious Mahogany zone into the lower aquifers and then upward through the Mahogany zone and upper aquifers to the major streams. In some areas, ground water also discharges as springs. The general direction of ground-water movement is toward the north beneath the drainage basins of Piceance and Yellow Creeks.

A flow-system analysis in the drainage basins of Piceance and Yellow Creeks is based on potentiometric-head distributions described by Weeks and others (1974) and Robson and Saulnier (1981). The bedrock aquifers, valley-fill alluvial aquifers, Piceance Creek, and Yellow Creek are stream-aquifer systems in which the exchange of ground and surface water is possible. In the drainage basins of Roan and Parachute Creeks, the flow system is different because stream valleys are incised below the base of the lower aquifers. Recharged water moves through the upper aquifers, the Mahogany zone, and lower aquifers to seepage faces or springs above the streams, as shown in figure 5. The general direction of ground-water movement is toward the incised stream valleys. The stratigraphic location of seepage faces and springs is not completely understood because talus deposits cover parts of the canyon walls in the incised valleys. Water that discharges contributes to streamflow or is consumed by evapotranspiration. A flow-system analysis of Roan and Parachute Creeks valleys was based on measurements of potentiometric levels in a small number of existing wells, several aquifer tests by consulting firms, and observations of seepage faces and springs. Bedrock aquifers of the Uinta and Green River Formations and streams in Roan and Parachute Creeks basins are not stream-aquifer systems because streams are below the bases of these formations and cannot contribute water to the bedrock aquifers.

MATHEMATICAL MODEL

Two mathematical models for parts of Piceance basin have been prepared by the U.S. Geological Survey. A hydraulic model described by Weeks and others (1974) simulated the hydrologic system underlying the drainage basins of Piceance and Yellow Creeks. This quasi-three-dimensional model solved coupled two-dimensional flow equations for the upper and lower aquifers. Each aquifer was subdivided into about 800 nodes of variable spacing. Anisotropic hydraulic conductivity was not suspected and was not simulated. The model was used to study steady-state conditions and transient conditions caused by hypothetical mine drainage at tracts C-a and C-b. The second model was a hydraulic and transport model described by Robson and Saulnier (1981) and also prepared for the hydrologic system underlying the drainage basins of Piceance and Yellow Creeks. This model employs the five-layer subdivision shown in figure 3. Each layer was subdivided into a 9 X 14 array of variably spaced nodes that incorporated the estimated anisotropic variations in hydraulic conductivity. This model was used to appraise the hydraulic characteristics and chemical transport under steady-state conditions and transient conditions caused by hypothetical mine drainage at tracts C-a and C-b.

Model Framework and Hydrologic Parameters

The model that was selected for this study was a finite-difference model capable of simulating three-dimensional flow (Trescott, 1975; Trescott and Larson, 1976). The required model had to simulate the interactions between adjacent aquifers of different hydrologic characteristics and the interconnected streams in the Piceance and Yellow Creek drainages. The model uses a variable grid of block-centered nodes in a layered structure. The aquifer systems simulated may be heterogeneous and anisotropic and may have irregular boundaries. The model uses the strongly implicit procedure to approximate the following equation:

$$\frac{\partial}{\partial x}\left[T_{xx}\frac{\partial h}{\partial x}\right] + \frac{\partial}{\partial y}\left[T_{yy}\frac{\partial h}{\partial y}\right] + b\frac{\partial}{\partial z}\left[K_{zz}\frac{\partial h}{\partial z}\right] = S'\frac{\partial h}{\partial t} + bW(w,y,z,t), \quad (1)$$

where:

h=hydraulic head, or potentiometric head,
T_{xx}=principal component of transmissivity tensor in the x direction,
T_{yy}=principal component of transmissivity tensor in the y direction,
K_{zz}=principal component of hydraulic-conductivity tensor in the vertical (z) direction,
$W(x,y,z,t)$=volumetric flux per unit volume,
S'=storage coefficient,
x,y,z=space coordinates,
t=time coordinate or index, and
b=layer thickness.

The solution of the equation requires that the principal coordinate axes of the grid be aligned with the principal directions of the transmissivity. Initially the x axis of the grid was aligned N 75° W because of the predominance of surface fractures along this direction (fig. 4) and the suspected lateral anisotropy of transmissivity related to the fractures. The orientation and limit of the grid is shown in figure 6. The grid orientation permits a simulated increase or decrease in distributed values of transmissivity for any aquifer along rows of nodes (N 75° W) or along columns of nodes (N 15° E). Node widths ranged from 3,000 to 10,000 ft according to the needs for definition throughout the basin.

For simulation purposes, the bedrock aquifers and the confining layers were subdivided into the five layers listed below, which were shown graphically in figure 3.

Layer	Stratigraphic unit	Mean thickness (feet)
5	Uinta Formation----------	400
4	Green River Formation above Mahogany zone----------	300
3	Mahogany zone of Green River Formation----------	160
2	Green River Formation from base of R-6 oil-shale zone to base of Mahogany zone----------	190
1	Green River Formation from base of R-2 oil-shale zone to top of R-5 oil-shale zone----------	700

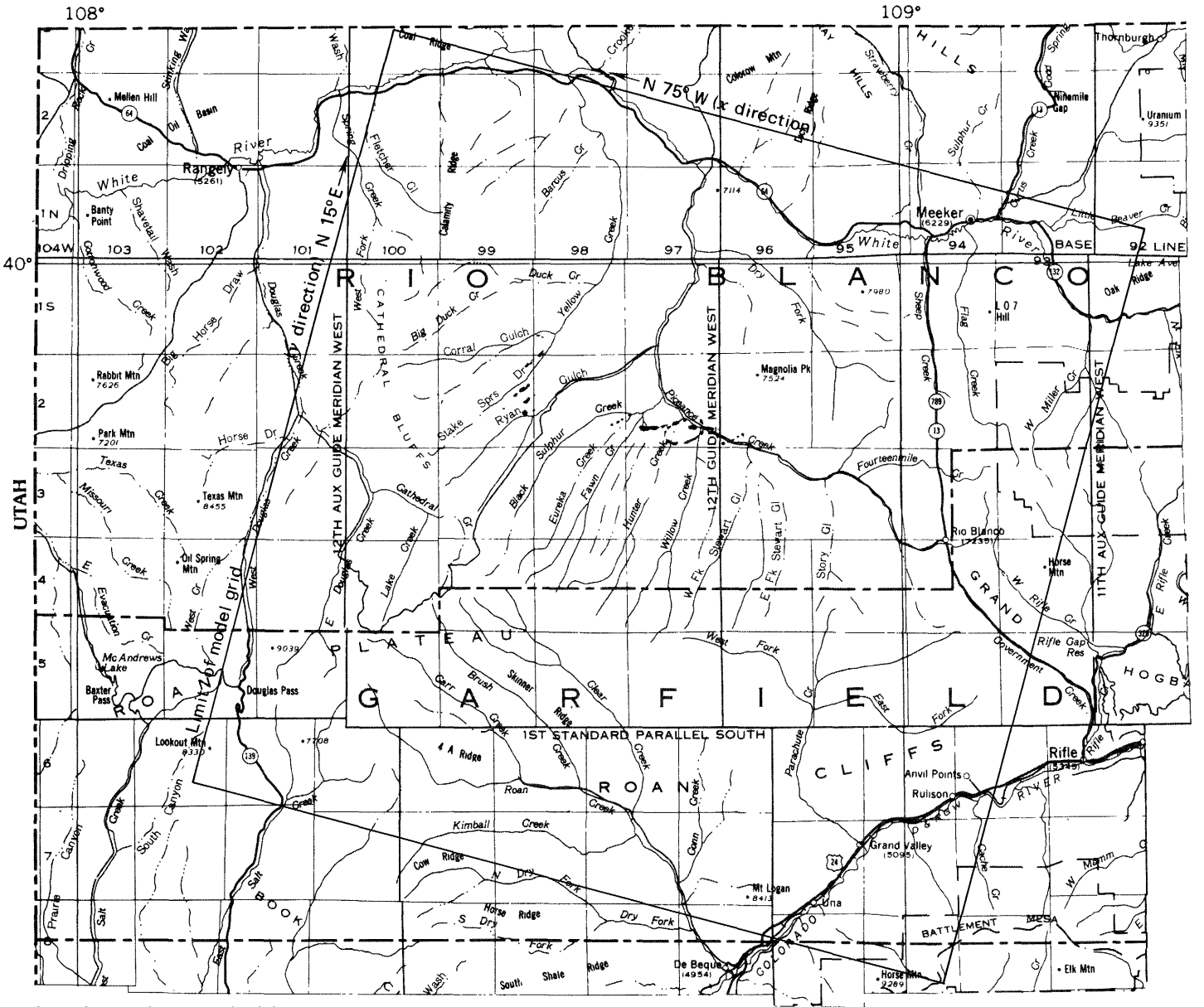

Figure 6.-- Orientation and limit of the initial grid for the mathematical model of the hydrologic system.

A similar five-layer subdivision was employed by Robson and Saulnier (1981), except that their layer numbers were reversed. Layers 1 and 2 often are called the lower aquifers; layers 4 and 5 often are called the upper aquifers. Layer 3 is the Mahogany zone, the confining layer that separates the lower aquifers and upper aquifers. The five-layer subdivision was utilized to allow a reasonable yet manageable degree of vertical definition of the flow system. The grid contains 40 rows and 46 columns, for a total of 9,200 nodes in all five layers. The model simulates the flow system within about 530 mi^3 of aquifers and confining beds in the Piceance basin. The constructed model was designed to account for lateral or vertical heterogeneity on a regional scale commensurate with the present existing and anticipated hydrologic data and predictions. A more detailed framework with additional rows, columns, and layers of the same region might become unwieldy, because of the requirement for additional computer storage, the expanded input-data requirements, and expanded data output.

Streams, seepage faces, and springs were simulated as constant-head nodes in the model. Piceance and Yellow Creeks were simulated as constant-head nodes in layer 5 in order to account for the stream-aquifer system. In the incised canyons of Roan and Parachute Creek basins, the base of layer 1 lies above the streams and the streams and aquifers are not hydraulically connected. Therefore, seepage faces and springs were simulated in the model as constant-head nodes but are not related to streamflow. Initially, the abundant seepage faces and springs along all incised canyons were simulated at an altitude of 7,200 ft for all layers. This altitude is an average for the various levels of discharge into incised canyons. Later simulations accounted for the altitudes of observed seeps and springs in layers 4 and 5 and presumed seeps and springs in layers 1 and 2 in each nodal location. (See section entitled, "Adjusted Model Design and Distributed Hydrologic Parameters.") Normally the steady-state solution used to locate seepage faces requires a trial-and-error search technique. This technique was not attempted because of uncertainties in the exact location and discharge of the seepage faces.

Previous and current attempts to quantify and simulate the hydrologic characteristics of the Piceance basin have been impaired by the lack of field data and the apparent heterogeneity of the characteristics. The hydrologic parameters summarized in table 1 were obtained from aquifer-test and simulated data described by Weeks and others (1974), Robson and Saulnier (1981); unpublished analyses of consulting and industrial firms; and estimates where parameter values were not available. Large ranges in hydraulic conductivity and transmissivity are probably due to variations in fracture aperture, density, and continuity. For the first model run, the estimated distributed values of transmissivity of aquifer layers also were increased directionally along the x axis of the grid (N 75° W) to account for suspected anisotropic transmissivity related to the fracture trends illustrated in figure 4. In addition the vertical hydraulic conductivities of all layers were reduced, compared to horizontal hydraulic conductivities, to account for the reported discontinuous nature of fractures in the vertical.

A heat-flow technique also was used to estimate the vertical hydraulic conductivity of the Mahogany zone. This method was proposed by Stallman (1960) and developed by Bredehoeft and Papadopulos (1965) and Sorey (1971). The technique requires a temperature log from a well tightly cemented across the Mahogany zone.

Table 1.--*Estimated hydrologic parameters of aquifer layers*

Layer	Stratigraphic interval	Average saturated thickness, in feet	Range in transmissivity, in foot squared per day		Range in vertical hydraulic conductivity, in feet per day		Ratio of horizontal hydraulic conductivity to vertical hydraulic conductivity
			From	To	From	To	
5	Uinta Formation----------	400	1	450	1.3×10^{-3}	5.6×10^{-1}	2.0
4	Green River Formation above Mahogany zone------	300	1	480	1.7×10^{-3}	8.0×10^{-1}	2.0
3	Mahogany zone of Green River Formation----------	160	5.3×10^{-2}	1.6×10^{1}	1×10^{-4}	3×10^{-2}	3.3
2	Green River Formation from base of R-6 oil-shale zone to base of Mahogany zone----------	190	1	220	3.9×10^{-4}	8.6×10^{-2}	13.4
1	Green River Formation from base of R-2 oil-shale zone to top of R-5 oil-shale zone----------	700	1	400	9.5×10^{-5}	3.8×10^{-2}	15.0

No vertical flow of water within the casing is permitted in this analysis. The fluid temperature in a test well in sec. 20, T. 1 N., R. 98 W. (Welder and Saulnier, 1978) is shown in figure 7. The downward curvature of the temperature log across the Mahogany zone suggests downward movement of ground water that distorts the temperature profile by moving relatively cool water into relatively warm-water zones. The indicated downward movement is confirmed by a downward hydraulic gradient, calculated using head data from two nearby wells, one completed above and the other completed below the Mahogany zone. The vertical hydraulic conductivity of the Mahogany zone was calculated at six sites using the data reported by Welder and Saulnier (1978).

Required data on the thermal conductivity of the Mahogany zone were obtained from Tihen and others (1968). Their study indicated a curvilinear relation between thermal conductivity perpendicular to bedding planes and the Fischer assay, a standard measure of oil-shale quality. For this analysis, the oil assay near the test wells (Pitman and Johnson, 1978) was used with the curvilinear relation to estimate the local thermal conductivity. The resulting hydraulic conductivities, which were calculated using the thermal conductivities and associated data, are shown in table 2. Vertical hydraulic conductivities from tests 2 and 3 agree well with estimates of Robson and Saulnier (1981), but the other tests give hydraulic conductivities that differ significantly from their estimates, which were based on simulation analyses. Therefore, vertical hydraulic conductivities calculated from heat-flow techniques are of uncertain accuracy and were not incorporated into the simulation model. However, the technique may prove to be the best method of determining distributed values of the vertical hydraulic conductivity of the Mahogany zone when more wells are drilled and are available for testing.

Steady-State Error Analysis

A steady-state error analysis was conducted to assess the errors in model formulation, because of the uncertainty in the exact configuration of model boundaries and the distribution of natural recharge, discharge, and transmissivity. The preliminary model was constructed with the following characteristics: The hydrologic characteristics of the aquifers and the confining layer, transmissivity and hydraulic conductivity, were distributed in the basin over the entire extent of the outcrop or subcrop of each layer. These characteristics were estimated from data described by Robson and Saulnier (1981) and Weeks and others (1974), and from aquifer-test results reported by consulting firms. Piceance Creek and Yellow Creek were modeled as constant-head nodes in hydraulic connection with layer 5, the Uinta Formation. Springs and seepage faces in the Roan and Parachute Creek basins were modeled as constant-head nodes through which natural discharge occurred. Estimated natural recharge was designed to occur only above land-surface altitudes of 7,000 ft and was presumed to increase with altitude. The initial steady-state model runs indicated that all nodes representing streams and springs were gaining and that the basic assumptions about the regional-flow system were valid. The error analysis indicated several incorrect assumptions in model formulation, so the best estimated hydrologic characteristics are described later in this report.

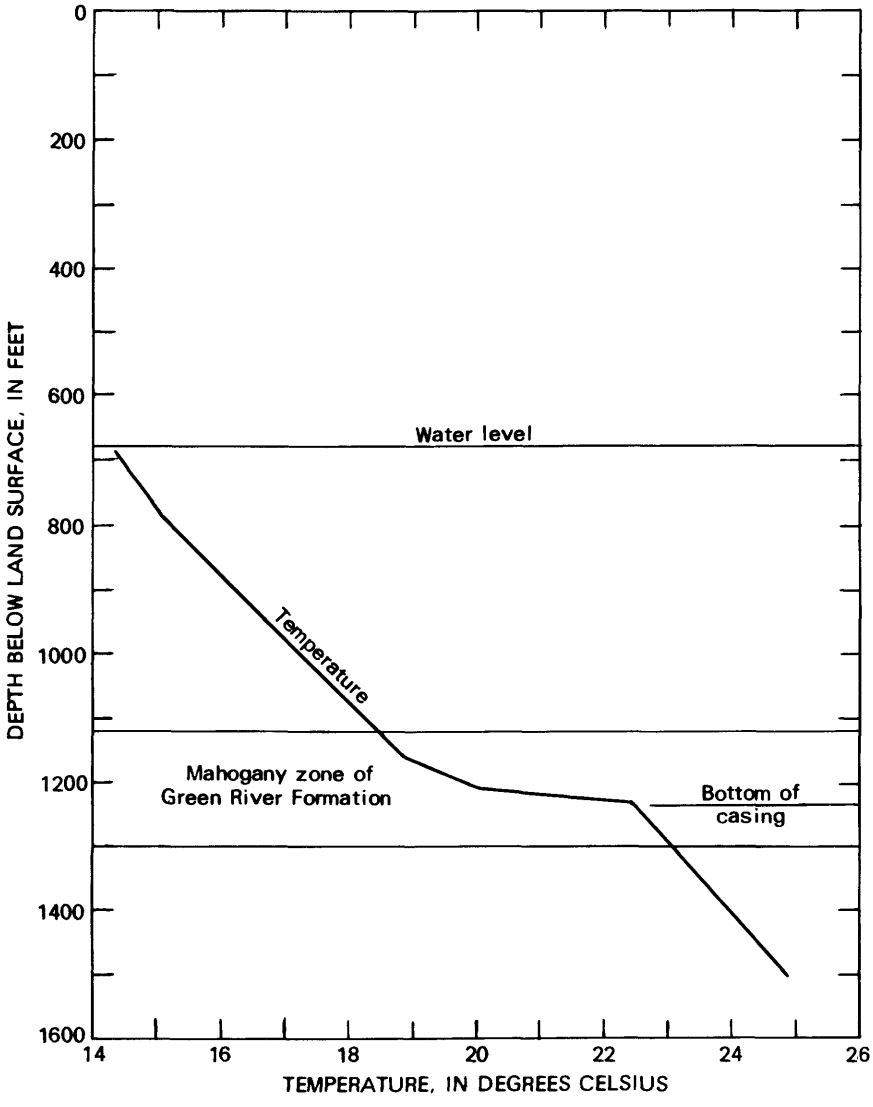

Figure 7.-- Fluid temperature in test hole in sec. 20, T. 1 N., R. 98 W., May 6, 1976 (Welder and Saulnier, 1978).

Table 2.--*Hydraulic and thermal characteristics of the Mahogany zone, Piceance basin, Colorado*

Test	Location	Thickness of zone analyzed (feet)	Hydraulic gradient, positive downward (foot per foot)	Average shale-oil concentration (Pitman and Johnson, 1978) (gallons per ton)	Estimated thermal conductivity (British thermal units per hour per foot per degree Fahrenheit)	Vertical velocity of water, positive downward (feet per day)	Vertical hydraulic conductivity (feet per day)	Thickness of overburden above Mahogany zone (feet)
1	sec. 30, T. 3 S., R. 97 W.	120	-0.14	28	0.62	-3.8×10^{-3}	2.8×10^{-2}	670
2	sec. 15, T. 2 S., R. 97 W.	125	.60	27	.64	1.9×10^{-3}	3.2×10^{-3}	875
3	sec. 20, T. 1 N., R. 98 W.	115	.88	18	.74	8.6×10^{-3}	9.7×10^{-3}	1,125
4	sec. 8, T. 2 S., R. 95 W.	190	.04	16	.79	1.6×10^{-3}	4.1×10^{-2}	1,200
5	sec. 14, T. 1 S., R. 96 W.	225	.02	17	.77	3.2×10^{-4}	1.3×10^{-2}	1,260
6	sec. 3, T. 2 S., R. 98 W.	210	.37	27	.64	2.9×10^{-4}	7.8×10^{-4}	1,195

The error analysis was conducted by changing various model parameters and observing the changes in the simulated head distribution in layers 1, 2, 4, and 5. Streamflow records were not used because of uncertain gains and losses in the streams. Predicted heads in the four layers were compared with measured heads in selected wells completed in various layers in the basin. The wells were selected to represent a network distributed over the basin rather than a cluster in one local region, in an attempt to minimize error throughout the three-dimensional flow field. The number of selected wells completed in each layer is shown below:

Layer	Number of well measurements
5----------	1
4----------	17
3----------	0
2----------	10
1----------	25
Total------	53

For each error analysis, the difference between computed and measured heads was tabulated as a set of errors. In order to evaluate both the mean error and scatter of errors, the mean square error was calculated. The mean square error is the sum of the mean error squared and the variance of the errors. The mean error alone would not indicate errors accurately, because a small mean error might indicate nearly equal amounts of positive and negative errors. Conversely a small variance might indicate a small scatter of errors about a large mean error. Therefore the errors were analyzed using the mean square error, in order to minimize the mean error and variance of error. A schematic diagram of various combinations of the mean error and variance of error is shown in figure 8. By selecting a model with the smallest mean square error in a series of trials, the errors in the head distribution in the three-dimensional flow field will be minimal. The mean square error is sensitive to a small number of outlying errors that may increase the variance greatly and also affect the mean error. Therefore, a correctly formulated model and accurate field data are required to reduce the mean square error to a low level.

The mean square errors for 40 error trials were calculated. Most hydrologic parameters were varied over the entire basin and over the ranges of suspected uncertainty. The sensitivity of individual trials is probably partly related to the number of wells in the layer in which the parameter is varied, even though single-layer changes in the model tend to propagate through other layers. Other sources of error include:

1. Errors in model formulation.
2. Errors in hydrologic parameters.
3. Lateral differences between well location and node center in the model.
4. Errors in identifying the layer(s) in which a well is completed.
5. Vertical differences of water levels within individual layers that are due to vertical hydraulic gradients and are not calculated by the model.
6. Erroneous measurements of water levels in wells.

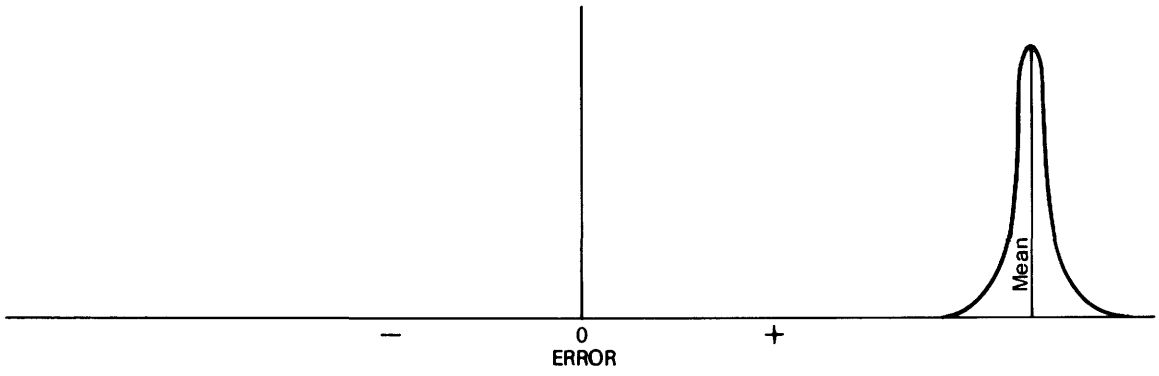

A. ERROR DISTRIBUTION WITH LARGE MEAN VALUE AND SMALL VARIANCE

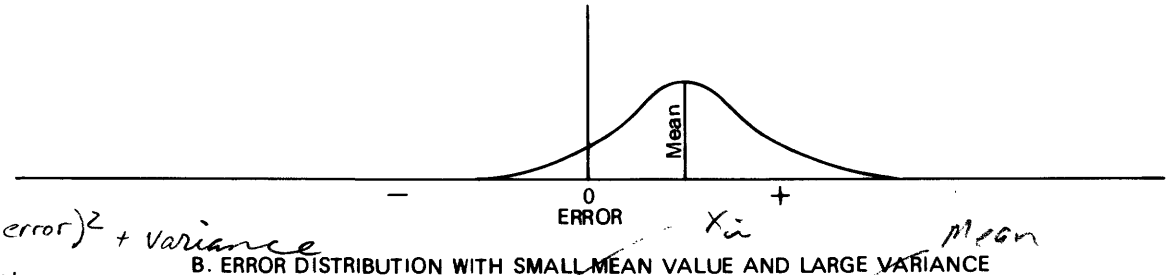

B. ERROR DISTRIBUTION WITH SMALL MEAN VALUE AND LARGE VARIANCE

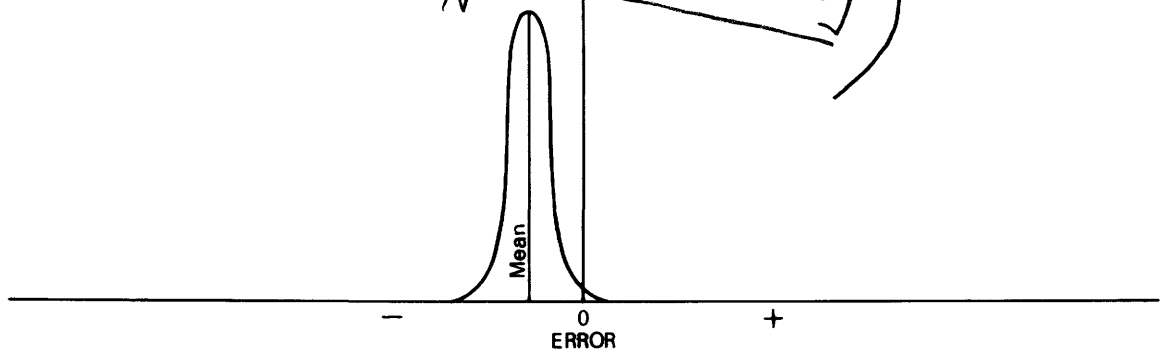

C. ERROR DISTRIBUTION WITH SMALL MEAN VALUE AND SMALL VARIANCE

Figure 8. -- Schematic diagram indicating various combinations of mean error and variance of error.

In spite of known weaknesses in the error analysis, the results were consistent. The simulated change of a single hydrologic parameter resulted in simulated head changes of hundreds of feet, in some cases. Furthermore, progressive changes in parameters induced progressive changes in values of the mean square error. Therefore the error analysis was used as a sensitivity technique for assessing the general and regional plausibility of the model framework and the hydrologic parameters.

Details of each error analysis are listed in table 3, and the mean square errors are plotted in figure 9. The standard, trial 1, simulated a steady natural recharge totaling 37.4 ft^3/s that discharged to Piceance and Yellow Creeks and the seepage faces in the drainage basins of Roan and Parachute Creeks. The estimated anisotropic characteristics of model layers that were used in trial 1 are shown in the tabulation below. For lateral anisotropy the transmissivity in the x direction, T_{xx}, is compared to transmissivity in the y direction, T_{yy}. For vertical anisotropy the vertical hydraulic conductivity, K_{zz}, is compared to the horizontal hydraulic conductivity, K_{xx}. However, the error analysis and field data indicated that several of these characteristics were wrong, as described later in this report.

Layer	Ratio of T_{xx} to T_{yy}	Ratio of K_{xx} to K_{zz}
5	3.0	2.0
4	2.0	2.0
3	1.0	3.3
2	2.0	13.4
1	2.0	15.0

For trial 1, the mean error was -22.16 ft, the variance was 38,640 ft^2, and the mean square error was 39,130 ft^2. Adjustments in the basinwide natural recharge in trials 2 and 3 produced higher errors than in trial 1.

Various hydrologic characteristics of individual layers were adjusted in trials 4 through 34. Simulated increases and decreases in basinwide transmissivity produced higher mean square errors. Increases and decreases in the vertical hydraulic conductivity also produced higher errors. The vertical hydraulic conductivity was increased so that the ratio of horizontal hydraulic conductivity to vertical hydraulic conductivity was 1.0 (compare to ratios in table 1). The vertical hydraulic conductivity also was reduced by a factor of 100. In trial 19, the reduction of the vertical hydraulic conductivity of the Mahogany zone resulted in the largest error of all trials. It appears that the 100-fold basinwide reduction of vertical hydraulic conductivity for this layer is not reasonable. In trial 20, the vertical hydraulic conductivity of the Mahogany zone was varied inversely with overburden thickness. This trial was designed to test the theory that the vertical hydraulic conductivity of the Mahogany zone is low where the zone is deeply buried, because of plastic deformation of the zone that could close fractures.

Table 3.--*Results of a steady-state error analysis of the ground-water system*

Trial	Simulated change	Mean square error (feet squared)
1	Standard	39,130
2	Recharge times 1.2	44,063
3	Recharge times 0.8	49,370
4	T_{xx}, T_{yy}, K_{zz} times 2.0 for layer 5	43,890
5	T_{xx}, T_{yy}, K_{zz} times 0.5 for layer 5	41,027
6	K_{zz} times 2.0 for layer 5	39,119
7	K_{zz} times 0.01 for layer 5	42,805
8	T_{xx} times 2.0 for layer 5	43,777
9	T_{xx}=T_{yy} for layer 5	37,134
10	Interchange T_{xx} and T_{yy} for layer 5	34,330
11	T_{xx}, T_{yy}, K_{zz} times 2.0 for layer 4	69,242
12	T_{xx}, T_{yy}, K_{zz} times 0.5 for layer 4	55,616
13	K_{zz} times 2.0 for layer 4	40,116
14	K_{zz} times 0.01 for layer 4	40,711
15	T_{xx} times 2.0 for layer 4	59,916
16	T_{xx}=T_{yy} for layer 4	32,536
17	Interchange T_{xx} and T_{yy} for layer 4	29,639
18	K_{zz} times 3.3 for layer 3	42,664
19	K_{zz} times 0.01 for layer 3	98,197
20	K_{zz} for layer 3 varies inversely with overburden thickness over layer 3	40,657
21	T_{xx}, T_{yy}, K_{zz} times 2.0 for layer 2	41,497
22	T_{xx}, T_{yy}, K_{zz} times 0.5 for layer 2	41,199
23	K_{zz} times 13.4 for layer 2	40,065
24	K_{zz} times 0.01 for layer 2	47,947
25	T_{xx} times 2.0 for layer 2	41,914
26	T_{xx}=T_{yy} for layer 2	39,891
27	Interchange T_{xx} and T_{yy} for layer 2	37,751
28	T_{xx}, T_{yy}, K_{zz} times 2.0 for layer 1	44,723
29	T_{xx}, T_{yy}, K_{zz} times 0.5 for layer 1	43,918
30	K_{zz} times 15.0 for layer 1	39,853
31	K_{zz} times 0.01 for layer 1	64,409
32	T_{xx} times 2.0 for layer 1	44,992
33	T_{xx}=T_{yy} for layer 1	37,989
34	Interchange T_{xx} and T_{yy} for layer 1	35,838
35	Interchange T_{xx} and T_{yy} for all layers	37,428
36	Reverse and double lateral anisotropy for layers 5, 4, 2, and 1	94,774
37	T_{yy}=3.40 T_{xx} for layers 4 and 5	55,140
38	T_{yy}=2.0 T_{xx} for layers 4 and 5	26,645
39	T_{yy}=3.40 T_{xx} for layer 4; T_{xx}=T_{yy} for other layers	47,875
40	T_{yy}=2.0 T_{xx} for layer 4; T_{xx}=T_{yy} for other layers	25,889

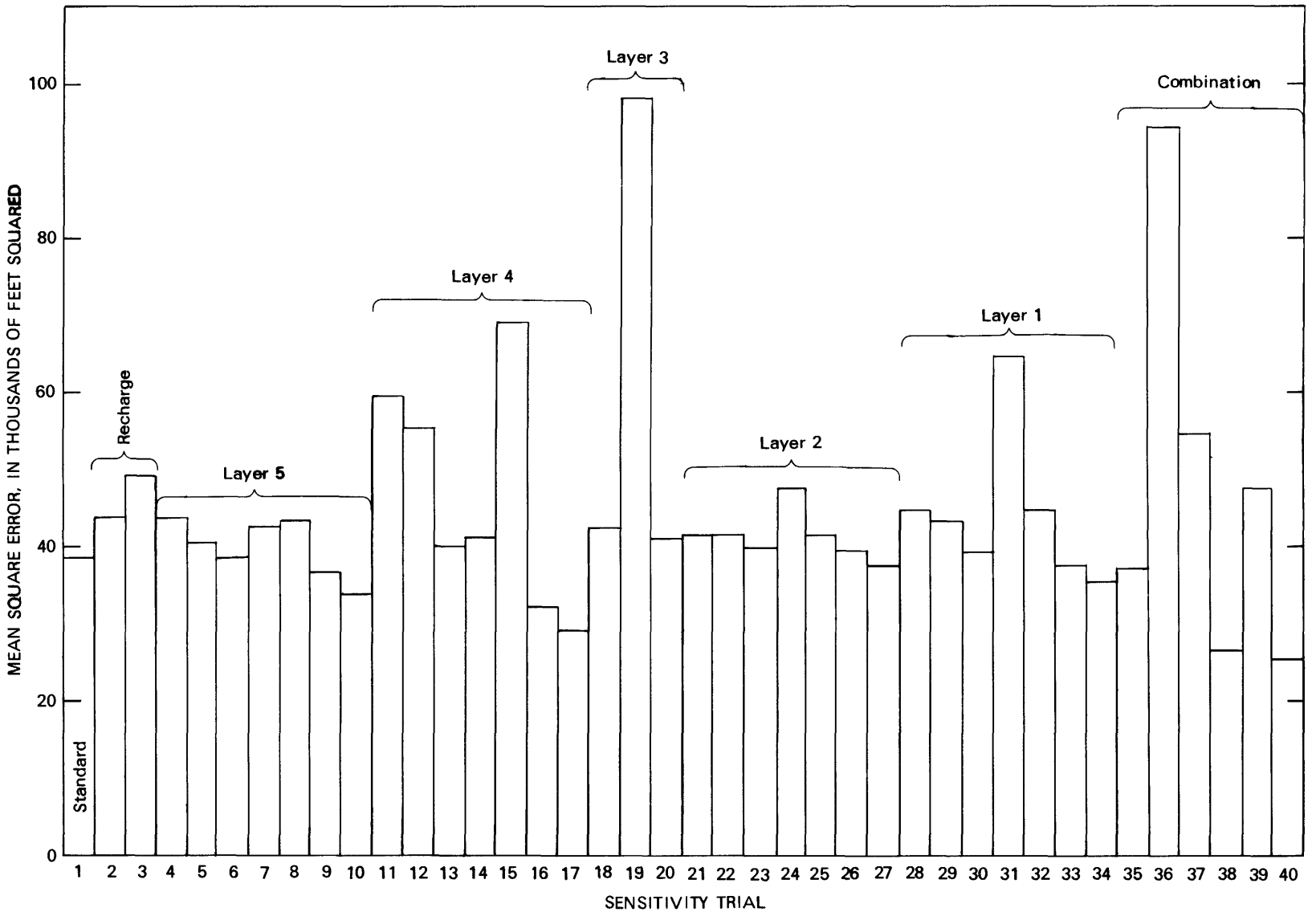

Figure 9.-- Mean square error for error analysis.

The most informative error trials were 8 through 10, 15 through 17, 25 through 27, and 32 through 34. These trials increased, eliminated, or reversed the lateral anisotropy of the transmissivity of the individual aquifer layers. For each layer, a higher error was indicated for an increase in transmissivity in the x direction (N 75° W). A lower error was indicated when the transmissivities were equalized along the trend of N 15° E, the y direction, and N 75° W, the x direction. When the transmissivities in the y direction (N 15° E) in each layer were increased in comparison to the transmissivities in the x direction (N 75° W), the error was reduced further. Apparently the fractures observed on the land surface do not extend at depth, or fracture aperture, spacing, or continuity dominate permeability more than the fracture trends observed on the land surface.

Trials 35 through 40 were designed after considering the evolving errors obtained in previous trials. These additional trials probed various combinations of the lateral anisotropy of the transmissivity. The ratio of 3.40 for T_{yy}/T_{xx} tested in trials 37 and 39 was derived from an aquifer test described in the following section of this report entitled Anisotropy of Hydraulic Conductivity. The trial yielding the greatest reduction in error was trial 40, in which the lateral anisotropy of the transmissivity in only layer 4 was reversed and the other layers were made laterally isotropic. The resulting mean square error was 25,889 ft^2, a 34-percent reduction of the error in trial 1. The measured and simulated altitudes of the potentiometric surface in wells are compared for trial 40 in table 4. The locations of well measurements used for the error analysis are shown in figure 10. Single wells with more than one measurement indicate multiple completion of a well or successive water-level measurements during well drilling. The striking difference between the inferred axis of major transmissivity of layer 4 and the trend of surface fractures shown in figure 4 prompted additional analysis of aquifer anisotropy, as described in the following section.

Anisotropy of Hydraulic Conductivity

The directional transmissivity detected during steady-state modeling was investigated further because of its importance in the response of the hydrologic system to pumping or injection. Directional transmissivity must be due to directional hydraulic conductivity rather than the aquifer thickness, because thickness cannot vary radically with direction at any site.

Additional information on the directional hydraulic conductivity of the upper aquifers was obtained from industrial withdrawals of water from beneath tract C-b (fig. 2). Reasonably steady withdrawals near shafts in the tract induced drawdown in observation wells that was analyzed using the techniques of Papadopulos (1965). Results from the 24-day test were analyzed, using three observation wells located within 127 ft of the pumped well. Analysis of data from these observation wells suggested another possible major axis of transmissivity. The resulting major axis of local transmissivity was N 3° W along which transmissivity of the upper aquifers was calculated as 320 ft^2/d. The local transmissivity along the orthogonal minor axis (N 87° E) was 94 ft^2/d. The local ratio of the transmissivity along the major axis to the transmissivity along the minor axis was 3.40.

Table 4.--*Comparison of measured and simulated altitudes of the potentiometric surface in 53 wells for trial 40 of error analysis*

Well measurement	Altitude of potentiometric surface, in feet		Error, in feet
	Measured	Simulated	
	LAYER 5		
38	7,388.	7,188.15	-199.85
	LAYER 4		
3	6,136.20	6,248.22	112.02
5	5,935.14	5,939.34	4.20
9	6,229.68	6,211.52	-18.16
13	6,682.70	6,280.29	-402.41
15	6,159.80	6,404.17	244.37
16	6,576.92	6,522.66	-54.26
17	6,272.20	6,294.84	22.64
20	6,332.69	6,437.96	105.27
22	6,316.0	6,248.26	-67.74
25	6,598.05	6,384.72	-213.33
26	6,901.80	6,657.81	-243.99
32	6,759.15	6,828.51	69.36
36	7,345.	7,187.37	-157.63
40	8,091.90	7,831.14	-260.76
43	8,041.90	7,983.12	-58.78
44	8,031.40	7,962.15	-69.25
47	7,664.61	7,573.49	-91.12
	LAYER 2		
11	6,035.0	6,120.55	85.55
24	6,520.50	6,372.20	-148.30
27	6,894.50	6,648.79	-245.71
31	6,570.	6,700.44	130.44
34	6,487.57	6,591.22	103.65
37	7,318.	7,183.00	-135.00
42	7,527.	7,994.22	467.22
51	8,015.	8,082.48	67.48
52	8,600.	8,757.15	157.15
53	7,709.6	7,765.48	55.88

Table 4.--*Comparison of measured and simulated altitudes of the potentiometric surface in 53 wells for trial 40 of error analysis*--Continued

Well measurement	Altitude of potentiometric surface, in feet		Error, in feet
	Measured	Simulated	
	LAYER 1		
1	5,916.	6,060.32	144.32
2	6,033.90	6,240.90	207.00
4	5,909.99	5,943.94	33.95
6	6,058.75	6,058.65	-.10
7	6,629.	6,702.06	73.06
8	6,606.	6,582.60	-23.40
10	6,183.85	6,235.42	51.57
12	6,440.	6,263.80	-176.20
14	6,154.22	6,386.97	232.75
18	6,194.20	6,295.04	100.84
19	6,570.	6,895.18	325.18
21	6,320.41	6,430.83	110.42
23	6,241.1	6,247.40	6.30
28	6,958.	6,821.09	-136.91
29	6,952.	7,088.98	136.98
30	6,590.	6,703.51	113.51
33	6,775.70	6,833.49	57.79
35	7,072.90	6,909.47	-163.43
39	8,460.	8,463.24	3.24
41	7,757.70	7,743.06	-14.64
45	7,681.90	7,716.43	34.53
46	7,970.	7,815.01	-154.99
48	7,473.59	7,566.33	92.74
49	8,085.	8,124.97	39.97
50	8,460.	8,463.24	3.24

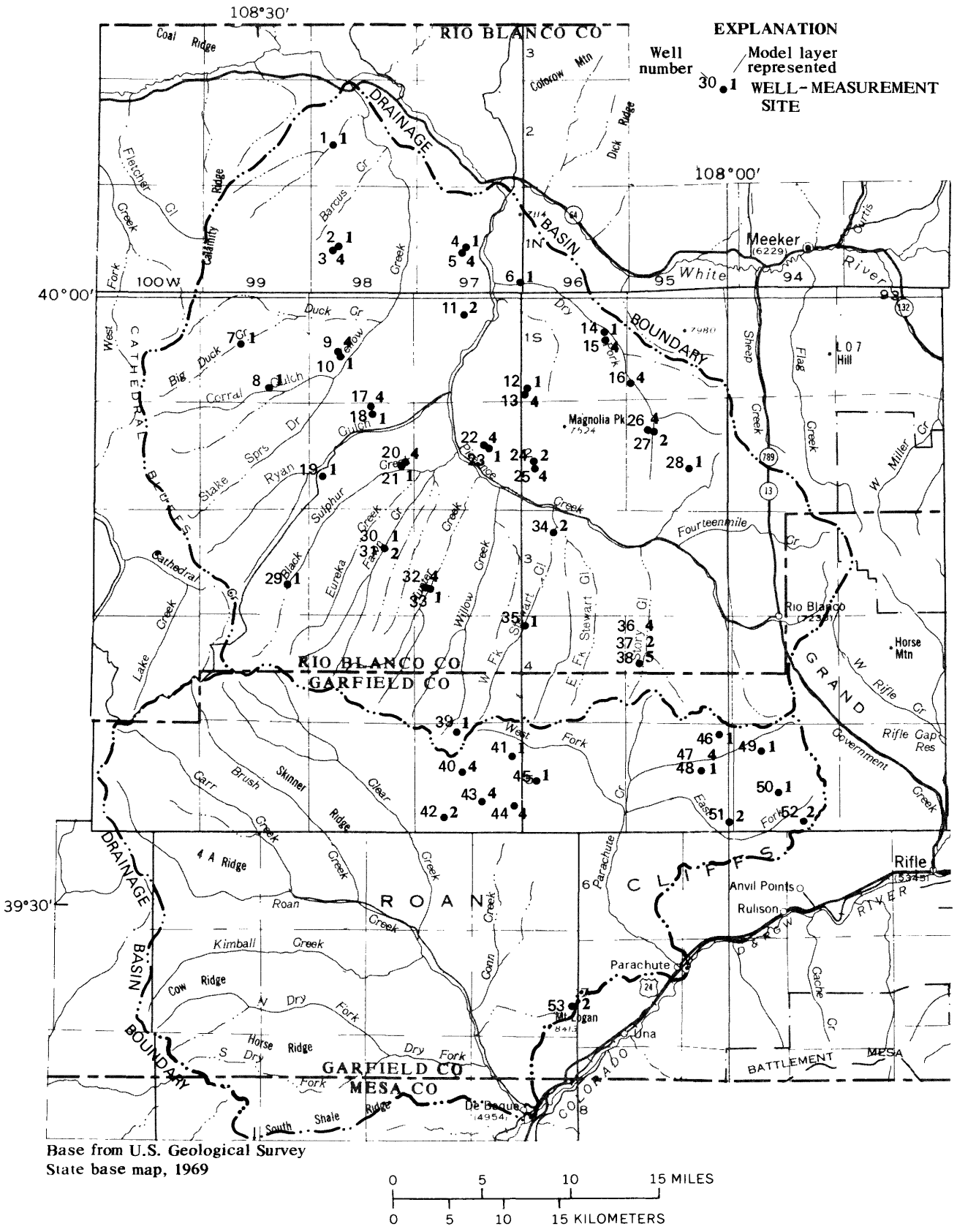

Figure 10.--Well measurements used for steady-state error analysis.

The effects of industrial withdrawals at tract C-a also were analyzed by plotting drawdown in all wells completed in the upper aquifers. The contoured drawdown cone is shown in figure 11. Pumping began on January 1, 1978, so the resulting cone shown in figure 11 is due to withdrawals that continued for more than 20 months. A small part of the withdrawn water was reinjected at several sites, but intermittently. The major axis of the drawdown cone, about N 15° W, indicates the major axis of hydraulic conductivity in the upper aquifers. The ratio T_{yy}/T_{xx} can be estimated by comparing the major and minor axes of the elliptical drawdown contours (Papadopulos, 1965, p. 24). However, the historical injection into the aquifer probably changed the drawdown pattern and therefore the ratio was not calculated.

The directional characteristics of the lower aquifers are even less known than the characteristics of the upper aquifers. Multiple-well aquifer tests in the lower aquifers are described by Loo and others (1979). Their results are described in table 5. The different trends of the major axes of transmissivity in the two zones and the similar values of the transmissivities along the major and minor axes in the two zones suggest that the lower aquifers are not particularly anisotropic in the lateral direction. Perhaps nondirectional solution channels control water movement more than directional fractures. The indicated ratios of horizontal to vertical hydraulic conductivity are similar to values reported by Robson and Saulnier (1981) and are listed in table 1.

Adjusted Model Design and Distributed Hydrologic Parameters

Information obtained from the error analysis and studies of the lateral anisotropy of hydraulic conductivity indicated that the initial model-grid orientation shown in figure 6 was not necessarily correct. Therefore, the model grid was reoriented so that the y axis was oriented N 15° W and the x axis was oriented N 75° E. Grid orientation was determined by the longitudinal axis of the drawdown cone shown in figure 11, the response to the largest pumping stress on the upper aquifer to date. The final model grid is shown on plate 1. The limit of bedrock aquifers coincides with the extent of the Parachute Creek Member (Weeks and others, 1974, pl. 1). Column widths range from 3,000 to 7,000 ft; row widths range from 4,000 to 10,000 ft. In order to provide more detailed solutions, a smaller column and row spacing was utilized in areas where development is expected. The entire grid of 40 columns, 46 rows, and 5 layers consists of 9,200 nodes; 3,115 nodes are outside the basin and 6,085 are used actively in the model analysis.

The constant-head nodes shown on plate 1 were used to simulate streams and seepage faces. The constant-head nodes shown along Yellow and Piceance Creeks and tributaries are located only in layer 5. These nodes were used to simulate the effects of streams hydraulically connected to the bedrock aquifers. Other constant-head nodes used to simulate seepage faces are located in layers 1, 2, 4, and 5.

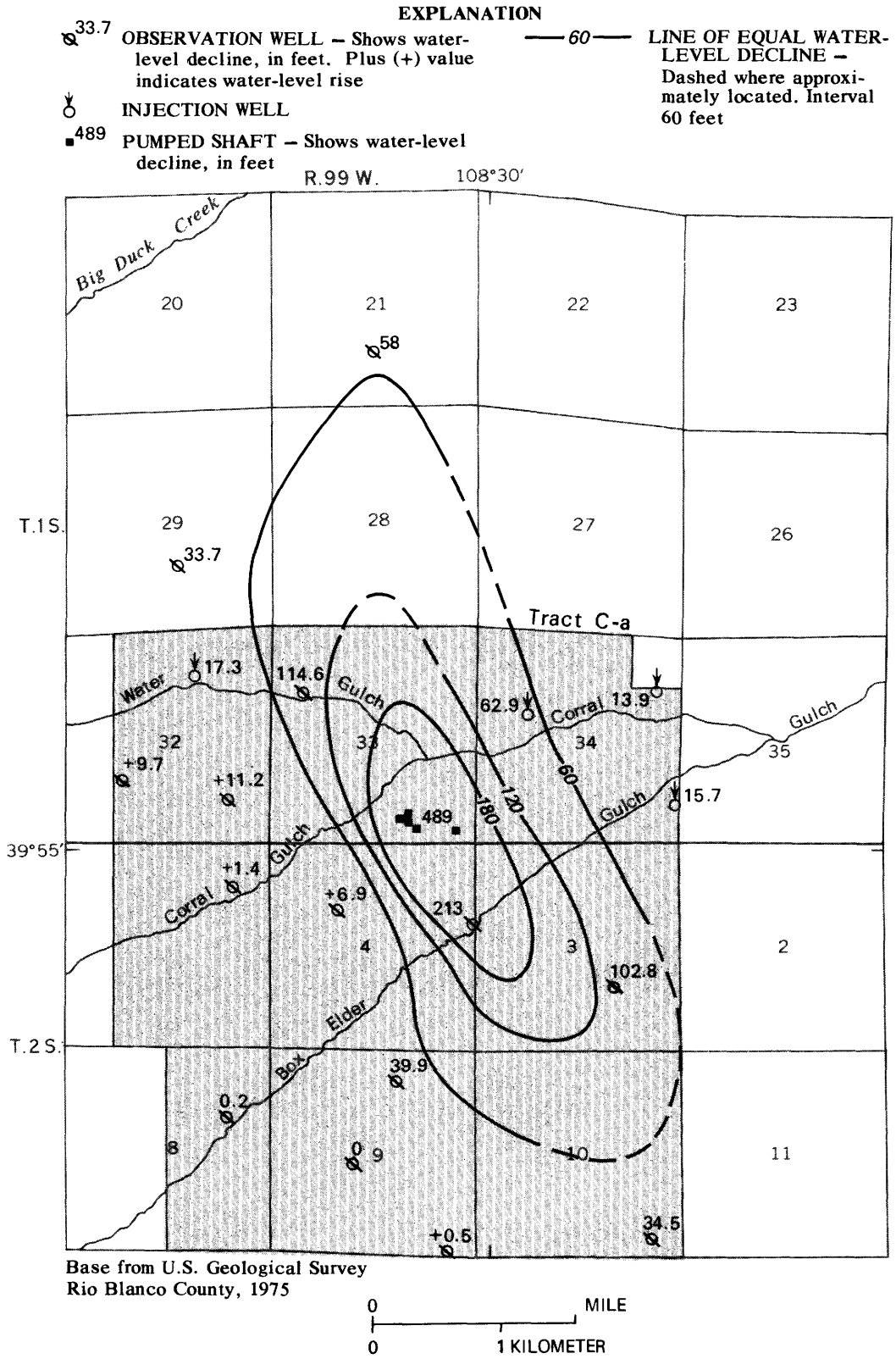

Figure 11.– Drawdown caused by industrial pumping of upper aquifer in tract C-a from January 1, 1978, to September 15, 1979.

Table 5.--*Anisotropic characteristics of the lower aquifers*

[From Loo and others, 1979]

Zone	Trend of major transmissivity	Major transmissivity (ft/d)	Minor transmissivity (ft/d)	Ratio of horizontal hydraulic conductivity to vertical hydraulic conductivity
Upper part of lower aquifers----	N 78° E	140	120	12.1
Lower part of lower aquifers----	N 73° W	130	120	16.6

An exception is East Fork Parachute Creek, where the constant-head nodes were only specified in layers 4 and 5. Seepage faces were not simulated in some south-facing slopes because of reports that seepage does not occur on these slopes. The altitudes of the seepage faces were estimated from structure contour maps and stratigraphic information. It was presumed that layers 4 and 5 discharge near the bases of the layers as observed in field studies. The location of the seepage faces of layers 1 and 2 is less certain because talus slopes often hide the faces. Therefore, seepage from layers 1 and 2 was presumed to discharge at the midpoint of the layers. The model includes a total of 358 constant-head nodes.

The mean square error also was determined for the head distributions predicted by the adjusted model. In addition, more extreme ratios of T_{yy}/T_{xx} for layer 4 were tested to ascertain that the ratio of 2.0 (see table 3, trial 40) represents the best value. Hantush (1966) has shown that the transmissivity ratio in a laterally anisotropic aquifer is sensitive to the trend of the orthogonal axes along which the ratio is calculated. The major transmissivity for layer 4 was presumed to trend N 15° E in the initial model; in the adjusted model the trend is N 15° W, a difference of 30 degrees. The mean square errors for six simulation trials are shown below:

Ratio of T_{yy} to T_{xx} for layer 4 in adjusted model	Mean square error (ft^2)
1.0	49,852
2.0	23,428
3.0	31,147
4.0	54,028
5.0	74,288
6.0	101,999

An additional simulation trial was made in which the ratio of T_{yy} to T_{xx} was 2.0 for layers 4 and 5, similar to trial 38 in table 3 for the initial model. The mean square error for this trial was 25,484 ft^2, which was greater than the error for the trial where only layer 4 was presumed laterally anisotropic. Apparently the suggested basinwide ratio of 2.0 for T_{yy}/T_{xx} for layer 4 is the best estimate at this stage of the analysis, even though no plausible explanation is obvious for the lateral anisotropy of this layer.

Several values of the mean square error were similar. These values resulted from trials using transmissivity ratios of 2.0 and 3.0 for layer 4 in the adjusted model and for a transmissivity ratio of 2.0 for the initial model (table 3, trial 40). The mean square errors for these trials are repeated for convenience.

Model	Ratio of T_{yy} to T_{xx} for layer 4	Mean square error (ft^2)
Adjusted---------	2.0	23,428
Adjusted---------	3.0	31,147
Initial----------	2.0	25,889

A statistical technique was used to test hypotheses about the transmissivity ratio and direction. The technique is an F-test and is described by Draper and Smith (1966, p. 274). Given the optimal transmissivity ratio for the adjusted model of 2.0, the hypothesis that the ratio is 3.0 was tested. This hypothesis was rejected at the 1-percent significance level, which indicates that there is only a 1-percent chance of obtaining the transmissivity ratio of 2.0 if the actual transmissivity ratio were really 3.0. The statistical technique also was used to test the hypothesis that the direction of major transmissivity for layer 4 is N 15° E (initial model) rather than N 15° W (adjusted model). This hypothesis was rejected at the 10-percent significance level, which indicates that there is only a 10-percent chance of obtaining the major direction of transmissivity along N 15° W, if the actual direction were really N 15° E, based on the available water-level information. These statistical techniques presume that the heads are representative of the layers penetrated and are normally distributed within each layer. Therefore, although the axes are statistically different, the transmissivity ratio and the true direction of the major axis of transmissivity cannot be well known until additional water-level, aquifer test, and geologic data are collected. Additional field data may indicate that the selected model characteristics are erroneous or only partly correct because the mean square error of 23,428 ft^2 for the selected model indicates a large error persists. The individual errors were plotted on maps to search for patterns in errors; no systematic pattern was observed throughout the basin. The lowest error obtained using the adjusted model is less than the lowest error obtained using the initial model. However, the model cannot be considered calibrated until assumed hydrologic characteristics are verified by detailed field studies. These characteristics are especially uncertain in the drainage basins of Roan and Parachute Creeks.

The estimated hydrologic characteristics of the five layers are summarized on plates 2 through 6. These characteristics are derived from Robson and Saulnier (1981), consultants' unpublished reports, information described herein, and estimates. Transmissivities of various layers are shown on plates 2, 3, 5, and 6, and appear to be relatively high near Piceance Creek compared to the rest of the basin. Layer 4 exhibits lateral anisotropy as previously discussed and portrayed by the inset block diagram showing relative hydraulic conductivity on plate 3. The indicated transmissivity of layer 4 is the lateral transmissivity T_{xx} and must be doubled to determine the transmissivity T_{yy} in the direction of N 15° W. Layers 1, 2, 3, and 5 were assumed to be laterally isotropic.

The estimated vertical hydraulic conductivity of layer 3, rather than the transmissivity, is shown on plate 4 because the vertical movement of water is more important than the lateral movement in this layer. The vertical hydraulic conductivity of layer 3 is based mostly on simulation studies and is not well known. Directional relative hydraulic conductivity is shown also in each figure. Each layer appears to exhibit reduced vertical conductivity compared to lateral conductivity. An estimated local value of lateral or vertical hydraulic conductivity that is not directly indicated on plates 2 through 6 may be calculated. Lateral hydraulic conductivity may be calculated by dividing transmissivity by saturated thickness (table 1). The diagram showing constant ratios of directional hydraulic conductivity for each figure may be used to estimate the hydraulic conductivity in one direction from a known hydraulic conductivity in another direction.

The amount of natural recharge estimated from precipitation is shown on plate 7. Values range from 0 at altitudes below 7,000 ft in the basin to about 3 in. per year at altitudes above 8,500 ft. Initial estimates of recharge in the northern part of the basin were derived from values estimated by Weeks and others (1974) using a watershed model, and by Robson and Saulnier (1981). Estimated values of recharge in the southern part of the basin, which were based on an estimated relation between precipitation and altitude, probably could be determined more accurately by means of watershed modeling. The final estimate of basinwide recharge was about 50 ft^3/s.

A steady-state simulation was made using the model that produced potentiometric-surface maps for all five layers. The resulting surfaces are similar for layers 4 and 5 and for layers 1 and 2. The potentiometric surface for layer 5 is shown on plate 8. Many of the contours cannot be verified because of the lack of hydrologic data, especially in the southern part of the basin. In the northern part of the basin, the water in bedrock aquifers drains to Piceance and Yellow Creeks. In the south, the water drains to seepage faces along the deeply incised valleys. The potentiometric surface does not indicate a ground-water drainage divide comparable to the surface drainage divide between the drainage basins of the White and the Colorado Rivers. Undoubtedly, the indicated flow patterns are strongly controlled by the low vertical hydraulic conductivities of the aquifer layers compared to lateral hydraulic conductivities. The computed potentiometric surface of layer 1, shown on plate 9, is similar to the surface of layer 5, except that in this layer steep potentiometric gradients are indicated along the incised valleys toward the low-lying seepage faces. Uncertainties in the potentiometric surfaces of all of the aquifer layers cannot be reduced until more hydrologic data are available.

The ground-water budget of the adjusted steady-state model is summarized in table 6. For comparison the measured mean discharge for January at the mouths of major streams is shown below:

Piceance Creek	22.8 ft^3/s
Yellow Creek	.86 ft^3/s
Roan and Parachute Creeks	28.1 ft^3/s

Presumably the January measurements represent baseflow conditions and exclude overland flow that is not considered in the model. However, the values of natural seepage in table 6 and stream discharge under low-flow conditions are not strictly comparable. Measured stream discharge includes the effects of surface runoff, ice storage, interchanges with underflow in alluvial aquifers, and transient flow components related to evapotranspiration and irrigation activities.

Table 6.--*Ground-water budget, estimated from steady-state model, in cubic feet per second*

Natural recharge		48.9
Natural discharge:		
Piceance Creek	23.9	
Yellow Creek	7.6	
Seepage:		
Layer 5	3.0	
Layer 4	7.1	
Layer 2	4.1	
Layer 1	3.2	
Total seepage	17.4	
Total discharge		48.9

CONCLUSIONS

A three-dimensional steady-state mathematical model containing five layers was prepared for the Piceance basin. Initial orientation of one grid axis was N 75° W parallel to a major fracture trend direction noted on the land surface. Lateral anisotropy was suspected with the transmissivity being greater in the direction of the major fracture direction. Initial model runs showed a large variation between model-generated heads and heads determined from well measurements. An error analysis using mean square error as a measure was used to evaluate the results of forty simulations. The lowest values of mean square error occurred when all layers had impaired vertical hydraulic conductivity and the lateral transmissivity of each layer was greater in the direction N 15° E, which is at right angle to the major fracture direction on the land surface. The lowest value of mean square error for all the trials was obtained when the lateral anisotropy was only in layer 4 and the other layers were laterally isotropic. The hydrogeological basis for only one layer being anisotropic and the others isotropic is not evident. As much as 200 ft of error between model-generated heads and heads determined from well measurements resulted from the simulation that had the lowest value of mean square error.

Simulation trials using a second grid orientation were made because of the possible anisotropy and the large amount of error that resulted from the initial simulations. The long axis of a pattern of elliptical drawdown contours from mine-shaft dewatering in the upper two layers in tract C-a were used to align a major axis of the grid. The orientation of the major axis is N 15° W and may represent a higher directional transmissivity than that along the trend of the minor axis. However, the shape of the drawdown contours may be affected by intermittent injection of the pumped water through wells present near or within the drawdown cone. Lowest values of mean square error resulted from simulations in which only layer 4 had a transmissivity ratio of 2:1 with the highest value along the direction of N 15° W. The results of the simulations with the two-grid orientatations suggest vertical impairment of flow in all layers and some degree of directional transmissivity in a northerly direction. The trend and the amount of directional transmissivity in each layer cannot be accurately determined with the data that are available.

Additional field data are needed to verify these preliminary conclusions. The model was not used for predictive purposes because of the lack of adequate hydrologic data in the basin.

FUTURE WORK NEEDS

Additional model analyses of the Piceance basin, particularly analyses of the hydrologic effects of draining numerous proposed oil-shale mines, will require:

1. Additional drilling and detailed aquifer testing at numerous sites.
2. Additional investigation of the stream-aquifer relations for Piceance and Yellow Creeks.
3. Additional investigation of discharge at seepage faces in relation to the flow system.
4. Additional investigation of natural recharge in the Roan and Parachute Creeks basins.
5. Continual adjustment of the hydrologic parameters used in the model and the model framework to insure that simulations are representative of the hydrologic system. An additional model layer to simulate the valley-fill alluvium is recommended to improve stream-aquifer relations during transient conditions.
6. Adaption of the model to improve simulation of extensive mine drainage. Required changes in the model include the ability to simulate the conversion from confined to unconfined aquifer conditions, adjustment in transmissivity to account for changes in saturated thickness of all layers, and simulation of stream and spring nodes as head-dependent discharge sites rather than constant-head nodes.

These recommended changes in the model will allow a meaningful analysis of the hydrologic effects of mine drainage and reinjection. The refined model will predict mine-drainage rates, drawdown in mines, the effects of well interference, and stream losses and gains due to mine drainage and reinjection.

REFERENCES

Bradley, W. H., 1931, Origin and microfossils of the oil shale of the Green River Formation of Colorado and Utah: U.S. Geological Survey Professional Paper 168, 58 p.

Bredehoeft, J.D., and Papadopulos, I.S., 1965, Rates of vertical groundwater movement estimated from the Earth's thermal profile: Water Resources Research, v. 1, no. 2, p. 325-328.

Cashion, W. B., and Donnell, J. R., 1972, Chart showing correlation of selected key units in the organic-rich sequence of the Green River Formation, Piceance Creek basin, Colorado and Uinta Basin, Utah: U.S. Geological Survey Oil and Gas Investigations Chart OC 65.

_____1974, Revision of nomenclature of the upper part of the Green River Formation, Piceance Creek basin, Colorado, and eastern Uinta Basin, Utah: U.S. Geological Survey Bulletin 1394-G, 9 p.

Coffin, D.L., Welder, F.A., and Glanzman, R.K., 1971, Geohydrology of the Piceance Creek structural basin between the White and Colorado Rivers, northwestern Colorado: U.S. Geological Survey Hydrologic Investigations Atlas HA-370.

Coffin, D.L., Welder, F.A., Glanzman, R.K., and Dutton, X.W., 1968, Geohydrologic data from Piceance Creek basin between the White and Colorado Rivers, northwestern Colorado: Colorado Water Conservation Board, Water-Resources Circular 12, 38 p.

Donnell, J. R., 1961, Tertiary geology and oil-shale resources of the Piceance Creek basin between the Colorado and White Rivers, northwestern Colorado: U.S. Geological Survey Bulletin 1082-L, p. 835-891.

Draper, N. R., and Smith, H., 1966, Applied regression analysis: New York, John Wiley, p. 274.

Federal Energy Administration, 1974, Potential future role of oil shale: Prospects and constraints: Final Task Force Report of Project Independence Blueprint, under direction of U.S. Department of the Interior, 495 p.

Hantush, M. S., 1966, A method for analyzing a drawdown test in anisotropic aquifers: Water Resources Research, v. 2, no. 2, p. 281-285.

Loo, W. W., Markley, D. E., and Dougan, P., 1979, Equity/DOE BX in situ oil shale project and three dimensional geohydrologic testing and analysis of the leached zone of the Green River Formation, Rio Blanco County, Colorado: Ninth Annual Rocky Mountain Groundwater Conference, Reno, Nev.

Papadopulos, I. S., 1965, Nonsteady flow to a well in an infinite anisotropic aquifer: International Association of Scientific Hydrology, Symposium of Dubrovnik, p. 21-31.

Pitman, J. K., 1979, Isopach, structure contour, and resource maps of the R-6 oil-shale zone, Green River Formation, Piceance Creek basin, Colorado: U.S. Geological Survey Miscellaneous Field Studies Map MF-1069.

Pitman, J. K., and Johnson, R. C., 1978, Isopach, structure contour, and resource maps of the Mahogany oil-shale zone, Green River Formation, Piceance Creek basin, Colorado: U.S. Geological Survey Miscellaneous Field Studies Map MF-958.

Robson, S. G., and Saulnier, G.J., Jr., 1981, Hydrogeochemistry and simulated solute transport, Piceance basin, northwestern Colorado: U.S. Geological Survey Professional Paper 1196, 65 p.

Smith, R. S., and Whitney, J. W., 1979, Map of joint sets and airphoto lineaments of the Piceance Creek basin, northwestern Colorado: U.S. Geological Survey Miscellaneous Field Studies Map MF-1128.

Sorey, M. L., 1971, Measurement of vertical groundwater velocity from temperature profiles in wells: Water Resources Research, v. 7, no. 4, p. 963-970.

Stallman, R. W., 1960, Notes on the use of temperature data for computing groundwater velocity: 6th Assem. Hydraul., Societe Hydrotechnique de France, Nancy, France, 1960, Rapp. 3, question 1, p. 1-7. (Also *in* Methods of collecting and interpreting ground-water data, Ray Bentall, compiler: U.S. Geological Survey Water-Supply Paper 1544-H, p. 36-46, 1963.)

Tihen, S. S., Carpenter, H. C., and Johns, H. W., 1968, Thermal conductivity and thermal diffusivity of Green River oil shale: National Bureau of Standards Special Publication 302, p. 529-535.

Trescott, P. C., 1975, Documentation of finite-difference model for simulation of three-dimensional ground-water flow: U.S. Geological Survey Open-File Report 75-438, 106 p.

Trescott, P. C., and Larson, S. P., 1976, Documentation of finite-difference model for simulation of three-dimensional ground-water flow: U.S. Geological Survey Open-File Report 76-591, 21 p.

U.S. Weather Bureau, 1960, Normal October-April precipitation, 1931-1960: Denver, Colorado Water Conservation Board, map.

Weeks, J. B., Leavesley, G. H., Welder, F.A., and Saulnier, G.J., Jr., 1974, Simulated effects of oil-shale development on the hydrology of Piceance basin, Colorado: U.S. Geological Survey Professional Paper 908, 84 p.

Welder, F. A., 1971, Map showing joint pattern inferred from aerial photographs: Denver, Water Resources in Colorado Oil Shale, Advisory Committee Study, Report on Economics of Environmental Protection for a Federal Oil-Shale Leasing Program, scale 1:380,000.

Welder, F. A., and Saulnier, G. J., Jr., 1978, Geohydrologic data from twenty-four test holes drilled in the Piceance basin, Rio Blanco County, Colorado, 1975-76: U.S. Geological Survey Open-File Report 78-734, 132 p.